

PHOTOACCLIMATION IN THE PHOTOTROPHIC MARINE CILIATE *MESODINIUM RUBRUM* (CILIOPHORA)¹

Holly V. Moeller,² Matthew D. Johnson³

Environmental Biophysics and Molecular Ecology Program, Institute of Marine and Coastal Sciences,
Rutgers University, 71 Dudley Road, New Brunswick, New Jersey 08901, USA

and Paul G. Falkowski⁴

Environmental Biophysics and Molecular Ecology Program, Institute of Marine and Coastal Sciences,
Rutgers University, 71 Dudley Road, New Brunswick, New Jersey 08901, USA

Department of Earth and Planetary Sciences, Rutgers University, 610 Taylor Road, Piscataway, New Jersey 08854, USA

Mesodinium rubrum (= *Myrionecta rubra*), a marine ciliate, acquires plastids, mitochondria, and nuclei from cryptophyte algae. Using a strain of *M. rubrum* isolated from McMurdo Sound, Antarctica, we investigated the photoacclimation potential of this trophically unique organism at a range of low irradiance levels. The compensation growth irradiance for *M. rubrum* was $0.5 \mu\text{mol quanta} \cdot \text{m}^{-2} \cdot \text{s}^{-1}$, and growth rate saturated at $\sim 20 \mu\text{mol quanta} \cdot \text{m}^{-2} \cdot \text{s}^{-1}$. The strain displayed trends in photosynthetic efficiency and pigment content characteristic of marine phototrophs. Maximum chl *a*-specific photosynthetic rates were an order of magnitude slower than temperate strains, while growth rates were half as large, suggesting that a thermal limit to enzyme kinetics produces a fundamental limit to cell function. *M. rubrum* acclimates to light- and temperature-limited polar conditions and closely regulates photosynthesis in its cryptophyte organelles. By acquiring and maintaining physiologically viable, plastic plastids, *M. rubrum* establishes a selective advantage over purely heterotrophic ciliates but reduces competition with other phototrophs by exploiting a very low-light niche.

Key index words: ciliate; *Geminigera cryophila*; karyoklepty; light limitation; *Mesodinium rubrum*; *Myrionecta rubra*; photoacclimation; quantum yield for growth

Abbreviations: PE, phycoerythrin; PI, photosynthesis versus irradiance

Unlike higher plants, eukaryotic algae can reversibly express components of the photosynthetic apparatus (Sukenik et al. 1988), including light-harvesting complexes and ratios of reaction centers (Falkowski

et al. 1981, Fujita et al. 1990, 1994) in response to changes in growth irradiance. This photoacclimation process is complex: the signals appear to be transduced by the redox poise of the electron transport chain (Escoubas et al. 1995) through a set of nested processes that optimize growth efficiency under varying irradiance levels (Falkowski and LaRoche 1991). Indeed, optimization of photosynthesis is directed toward a biophysical balance between the absorption of light and the generation of electrons for carbon fixation. This balance is achieved when the product of spectral irradiance (*E*) and the effective absorption cross-section of PSII (σ_{PSII}) equals the rate ($1/\tau$) at which electrons are photochemically extracted from water and used to reduce CO₂ (Falkowski and Raven 2007). This energetic balance requires close coordination between plastids (the information transduction processors) and the nucleus (the translational system)—with feedbacks. How this is achieved in a single algal cell remains unclear. Thus, the ability of a partial symbiont—a ciliate exploiting a cryptophyte alga—to photoacclimate is truly remarkable. The signals, which must be transferred across an intracellular matrix from the plastid to a specific nucleus and back, are either unrecognized by the host or are benignly guided. Here, we explore the physiology of photoacclimation in a symbiotic, but obligately phototrophic, ciliate.

The marine ciliate *M. rubrum* (also *M. rubra* and formerly *Cyclotrichium meunieri*) (Lohmann 1908, Jankowski 1976) is well known for its phototrophic capacity (Smith and Barber 1979, Stoecker et al. 1991, Johnson and Stoecker 2005, Johnson et al. 2006) and for its role in forming productive red tides in coastal and upwelling zones (Powers 1932, Bary and Stuckey 1950, Ryther 1967, Fenchel 1968). Following the discovery that *M. rubrum* requires cryptophyte prey for plastid maintenance and enhanced photosynthetic and growth rates (Gustafson et al. 2000), subsequent studies with the Antarctic strain demonstrated the novel trophic phenomenon of karyoklepty, or nuclear sequestration (Johnson et al. 2007). Retained cryptophyte

¹Received 24 May 2010. Accepted 13 September 2010.

²Present address: Department of Biology, Stanford University, 371 Serra Mall, Stanford, California 94305, USA.

³Present address: Woods Hole Oceanographic Institution, 266 Woods Hole Road, Woods Hole, Massachusetts 02543, USA.

⁴Author for correspondence: e-mail falko@marine.rutgers.edu.

nuclei in *M. rubrum* are transcriptionally active, apparently providing sufficient genetic information from the alga to synthesize chl and regulate plastid activity during intervals between feeding (Johnson and Stoecker 2005, Johnson et al. 2007). This phenomenon requires host-permitted expression of endosymbiont genes in the acquired algal nucleus and plastids.

Though debate exists in the literature over the degree of symbiosis, studies concur that *M. rubrum* must feed regularly to achieve maximal growth rates (Gustafson et al. 2000, Yih et al. 2004, Johnson and Stoecker 2005, Hansen and Fenchel 2006). However, feeding is a relatively rare life-cycle event (Yih et al. 2004), and the carbon contribution of prey cells is negligible compared to the amount of carbon fixed through photosynthesis (Johnson and Stoecker 2005, Smith and Hansen 2007). Therefore, *M. rubrum*'s feeding pattern supports its described ecological role as an obligate phototroph (Smith and Barber 1979, Laybourn-Parry and Perriss 1995, Gustafson et al. 2000, reviewed in Crawford 1989, but see Myung et al. 2006).

Photosynthesis in polar phytoplankton is controlled primarily by light and low temperatures at high latitude (Harrison and Platt 1986). Previous studies measured lower growth and photosynthetic rates in the polar *M. rubrum* strain than in its temperate counterpart, indicating that polar *M. rubrum* is kinetically limited by the cold temperatures to which it has adapted (Gustafson et al. 2000, Johnson and Stoecker 2005, Johnson et al. 2006). *M. rubrum* is also able to survive low-light polar winters, though cell densities drop dramatically and cells concentrate just beneath the ice cover to maximize exposure to any available light (Perriss et al. 1993, Gibson et al. 1997). Despite these stressful conditions, the ciliate does not form cysts during the overwintering period but instead retains high motility (Perriss et al. 1993, Gibson et al. 1997).

Multiple field and laboratory observations of coastal *M. rubrum* blooms have noted the ciliate's preference for low-intensity, diffuse light and its sensitivity to high light (Hart 1934, Bary and Stuckey 1950). The ciliate's tendency to aggregate in subsurface waters suggests that it positions itself in the water column based on thermal and irradiance cues (Owen et al. 1992). In Antarctic lakes, *M. rubrum* appears to exhibit a preference for low-light intensities (10%–50% of daylight), perhaps driven by competition with other phytoplankton (Laybourn-Parry and Perriss 1995). Baltic Sea *M. rubrum* populations can demonstrate a pronounced diel vertical migration (Lindholm and Mörk 1990) but frequently display maximum population densities at depth (Passow 1991, Olli and Seppälä 2001). Complex migratory patterns are probably related to a combination of requirements for light, cryptophyte prey, and nutrients. Therefore, low-light tolerance may not only be a response to polar conditions but may

also represent niche differentiation within the aquatic ecosystem. Antarctic ice algae often occur in dense mats and aggregations (Robinson et al. 1997), suggesting that cells arrange themselves to reduce incoming radiation by communal shading (Gibson et al. 1997). *M. rubrum* may also rely on the production of mycosporine-like amino acids (Johnson et al. 2006) and group shading in high-density blooms to reduce damage to individual cells from excess irradiance.

Here, we quantify the ability of *M. rubrum* to tolerate and acclimate to a range of light levels and measure photosynthetic performance by calculating the quantum yield for growth and carbon-fixation rates under different irradiance levels. Finally, we relate these photophysiological parameters to the bioenergetics of the ciliate's karyokleptic lifestyle.

MATERIALS AND METHODS

Growth of culture and experimental design. Cultures of *M. rubrum* (CCMP 2563) and *Geminigera* cf. *cryophila* (CCMP 2564), isolated from McMurdo Sound, Antarctica, in 1996 (Gustafson et al. 2000), were grown in 32 PSU F/2-Si media (Guillard 1975) in 1 L Ehrlenmeyer flasks at 4°C. Fiberglass screening and Cool White fluorescent bulbs (Philips Electronics, Andover, MA, USA) were used to obtain 10 experimental irradiance levels: $E_{\mu} = 0, 0.33, 1.7, 4.2, 8.6, 16, 33, 50, 75,$ and $100 \mu\text{mol quanta} \cdot \text{m}^{-2} \cdot \text{s}^{-1}$. Light intensity was measured with a QSL-100 light meter equipped with a 4π sensor (Biospherical Instruments Inc., San Diego, CA, USA). Healthy cells with a regular feeding history were acclimated to experimental irradiance levels for at least 1 week, and total culture volumes were brought to at least 350 mL with fresh F/2 media before measurements began. The ciliates were not fed during the course of the experiment.

Two independent trials of the photoacclimation experiment were performed. Each trial contained one culture incubated at each of the 10 experimental irradiance levels, for a total of 10 cultures per trial. Each of the two trials lasted 2 weeks, and all measurements were made on cells in exponential growth phase.

Measurement of growth rate, cellular health, and elemental content. Daily cell counts from each culture were taken using a Multisizer 3 Coulter Counter (Beckman Coulter Inc., Brea, CA, USA) fitted with a 70 μm aperture. Cell density on each day, for each culture, was calculated as the average of four replicate counts of aliquots fixed in 1% glutaraldehyde.

The average growth rate, μ_{avg} , was taken as the linear slope over the entire time course of the experiment, excluding initial time points corresponding to transfer acclimation. The zero growth limit, E_0 , was the x -intercept of the linear regression of growth rate on \ln (growth irradiance). The saturation point for growth, E_{sat} , was estimated as the point at which further increases in growth irradiance produced no significant gains in growth rate.

The quantum yield for photochemistry in PSII (F_v/F_m), a proxy for photosynthetic energy conversion efficiency, was measured daily with a Fluorescence Induction and Relaxation system (Satlantic Inc., Halifax, Nova Scotia, Canada). Quantum yield measurements were made on live culture aliquots after dark incubation on ice for 20 min. Weekly culture aliquots were collected on precombusted GF/F filters (Whatman Inc., Piscataway, NJ, USA), dehydrated, and analyzed for total carbon and nitrogen with an NA 1500 Series Z nitrogen/carbon/sulfur analyzer (Carlo Erba Instruments, Milan, Italy).

*Measurement of pigment content and chl *a* cross-section.* Chl *a* content was measured twice each week. Cells were filtered onto a Whatman GF/F filter, which was then placed in 90% acetone for 24 h (Parsons et al. 1984). An AMINCO DW-2000 UV-Vis spectrophotometer (SLM Instruments, Urbana, IL, USA) was used to obtain absorption spectra. The spectroscopic data were analyzed using the equations of Jeffrey and Humphrey (1975) for organisms containing chl *a* and chl *c* to determine chl *a* content.

Phycocerythrin (PE) was measured at the end of each experiment when cells were pelleted and immediately frozen at -80°C . The pellets were subsequently thawed and sonicated, and PE was extracted in 500 μL of seawater. Sample fluorescence was then measured using an EMax Precision Microplate Reader (Molecular Devices Inc., Sunnyvale, CA, USA). R-phycocerythrin (AnaSpec Inc. San Jose, CA, USA) was used to create a standard curve (linear relationship between fluorescence and PE concentration, $R^2 = 0.997$), and sample pigment concentrations were calculated.

The optical absorption cross-section normalized to chl *a* was measured by collecting an absorption spectrum of a suspension of cells from 375 to 750 nm using an AMINCO DW-2000 UV-Vis spectrophotometer. This absorption spectrum was then normalized to a cool-white fluorescence spectrum, as that of the bulbs under which cultures were grown. In conjunction with data on chl *a* content, an a_{chl}^* (mean chl *a*-specific spectral absorption [375–750 nm]) value representative of cross-section of each chl molecule in the cell was calculated using the equation:

$$a_{\text{chl}}^* = 100 \cdot S \cdot \ln(10) \cdot N \cdot C \quad (1)$$

where S is the normal sum, calculated from the absorption spectrum and light source emission spectrum; N is the concentration of *M. rubrum* in cells $\cdot \text{mL}^{-1}$; and C is the concentration of chl *a* in chl *a* $\cdot \text{cell}^{-1}$ (Dubinsky et al. 1984).

Determination of photosynthetic rate. Photosynthesis versus irradiance (PI) experiments were conducted at the end of each trial. Aliquots of each culture were removed, and a sample of each was fixed for a cell count in the manner described above. Aliquots were spiked with $\text{NaH}^{14}\text{CO}_3$ to a final concentration of $\sim 1 \mu\text{Ci} \cdot \text{mL}^{-1}$ (in trial 1) or $0.5 \mu\text{Ci} \cdot \text{mL}^{-1}$ (in trial 2). A total activity (TA) sample of 100 μL was added to 200 μL of β -phenylethylamine (Sigma-Aldrich, Corp., St. Louis, MO, USA), and a baseline (BL) sample of 2 mL was fixed in 200 μL of formaldehyde. Both TA and BL samples were refrigerated until the conclusion of PI measurements, when BL samples were acidified with 0.5 mL 6 N HCl. Immediately following addition of $\text{NaH}^{14}\text{CO}_3$, 1.5–2 mL subsamples were placed in 8 mL scintillation vials and incubated at 4.5°C – 6°C (temperature increased with irradiance) at 15 irradiance levels between 0 and $300 \mu\text{mol quanta} \cdot \text{m}^{-2} \cdot \text{s}^{-1}$ for 30 min. At the end of the incubation, samples were acidified with 0.5 mL 6 N HCl and placed with BL samples on a shaker table overnight at room temperature to remove excess bicarbonate.

After overnight acidification, 4 mL of UltimaFlo AP scintillation cocktail (PerkinElmer, Waltham, MA, USA) was added to all vials. Vials were vortexed to mix, and TA counts were made using an LS 6000IC Scintillation Counter (Beckman Coulter Inc.). Activity counts were converted to photosynthetic rates in either $\text{pg C} \cdot \text{cell}^{-1} \cdot \text{h}^{-1}$ or $\text{pg C} \cdot \text{chl a}^{-1} \cdot \text{h}^{-1}$ using the method described by Parsons et al. (1984). PI data for each acclimation level was fit using SigmaPlot 10.0 (Systat Software Inc., San Jose, CA, USA) to the hyperbolic tangent equation:

$$P = P_{\text{max}} \tanh(\alpha E / P_{\text{max}}) \quad (2)$$

where P is the photosynthetic rate measured at irradiance E (in $\mu\text{mol quanta} \cdot \text{m}^{-2} \cdot \text{s}^{-1}$), P_{max} is the maximum photosynthetic rate of the acclimation level, and α is the initial slope of light-limited photosynthetic rate. The irradiance at which

photosynthetic rate saturates is given by (Jassby and Platt 1976):

$$\frac{E_k = P_{\text{max}}}{\alpha} \quad (3)$$

Calculation of quantum yield for growth. The photosynthetic efficiency at different irradiance acclimations was calculated following the equation of Falkowski et al. (1985):

$$\phi_{\mu} = \frac{\mu \cdot 9.637 \times 10^{-4}}{a_{\text{chl}}^* \cdot (\text{chl } a/C) \cdot E_{\mu}} \quad (4)$$

where ϕ_{μ} is quantum yield for growth in $\text{mol C} \cdot \text{mol quanta absorbed}^{-1}$, chl *a*/C is the cellular chl to carbon ratio in $\text{mg chl } a \cdot \text{mg C}^{-1}$, 9.637×10^{-4} is a conversion constant (units of $\text{mol C} \cdot \text{d} \cdot \mu\text{mol quanta} \cdot \text{mg C}^{-1} \cdot \text{s}^{-1} \cdot \text{mol quanta}^{-1}$), and other parameters have been previously described.

RESULTS

Cell growth. Under saturating nutrient conditions and at a growth temperature of 4°C , *M. rubrum* achieved a maximum average growth rate (μ_{avg} ; see Table 1 for definitions of symbols used frequently in this paper) of 0.09 d^{-1} at the irradiance levels of 16 and $33 \mu\text{mol quanta} \cdot \text{m}^{-2} \cdot \text{s}^{-1}$ (Fig. 1). Inhibition of photosynthesis at higher irradiances was reflected by a decline in F_v/F_m (Fig. 1); the 10% decline in growth rates at the highest irradiance levels is due to photoinhibition. Growth rates saturated at an irradiance, E_{sat} , of $\sim 20 \mu\text{mol quanta} \cdot \text{m}^{-2} \cdot \text{s}^{-1}$. On the basis of regression analysis of $\ln(E_{\mu})$ on growth, we calculated a compensation irradiance for growth (E_0) of $\sim 0.5 \mu\text{mol quanta} \cdot \text{m}^{-2} \cdot \text{s}^{-1}$. Cultures incubated at irradiance levels below E_0 were excluded from subsequent calculations of photophysiological efficiency.

Cellular attributes. Cellular chl *a* concentration varied as a function of irradiance by a factor of 2.5. Cellular chl *a* content decreased as a logarithmic function of E_{μ} (Fig. 2, $r^2 = 0.98$), except for cultures incubated below E_0 , whose chl *a* $\cdot \text{cell}^{-1}$ decreased over the course of the experiment (data not shown). At high irradiance levels, cells produced less chl *a*, reducing the internal self-shading of each chl *a* molecule and increasing the chl *a*-specific optical absorption cross-section (a^* ; Fig. 2). Within our range of acclimation irradiances, a^* varied by a factor of 2.

PE content also varied with E_{μ} : cells acclimated to light levels of $16 \mu\text{mol quanta} \cdot \text{m}^{-2} \cdot \text{s}^{-1}$ or greater had lower cellular PE concentrations ($19.8 \pm 9.14 \text{ pg PE} \cdot \text{cell}^{-1}$) than lower light acclimations ($80.9 \pm 6.53 \text{ pg PE} \cdot \text{cell}^{-1}$) (Fig. 2). Cultures incubated below E_0 also had depressed PE content ($41.7 \pm 8.17 \text{ pg PE} \cdot \text{cell}^{-1}$). While the magnitude of cellular carbon ($\text{C} \cdot \text{cell}^{-1}$; units of $\text{ng C} \cdot \text{cell}^{-1}$) and nitrogen ($\text{N} \cdot \text{cell}^{-1}$; units of $\text{ng N} \cdot \text{cell}^{-1}$) varied across the two experimental replicates, C:N increased with increasing irradiance (Table 2).

Photophysiology. Photosynthetic rates and efficiency reflected a growth-irradiance-dependent transition from light limitation to light saturation. Trends in chl *a*-normalized maximum photosynthetic rate

FIG. 1. Growth rates and F_v/F_m (a proxy for photosynthetic health) plotted against the natural log of irradiance acclimation. Error bars represent standard deviation, $n = 2$. Cells were acclimated to a range of irradiance levels, and daily cell counts were made over 2-week incubation periods. Average growth rate (solid circles) increased linearly with $\ln(\text{growth irradiance})$ ($r^2 = 0.82$), while F_v/F_m (triangular symbols) had a sigmoidal response.

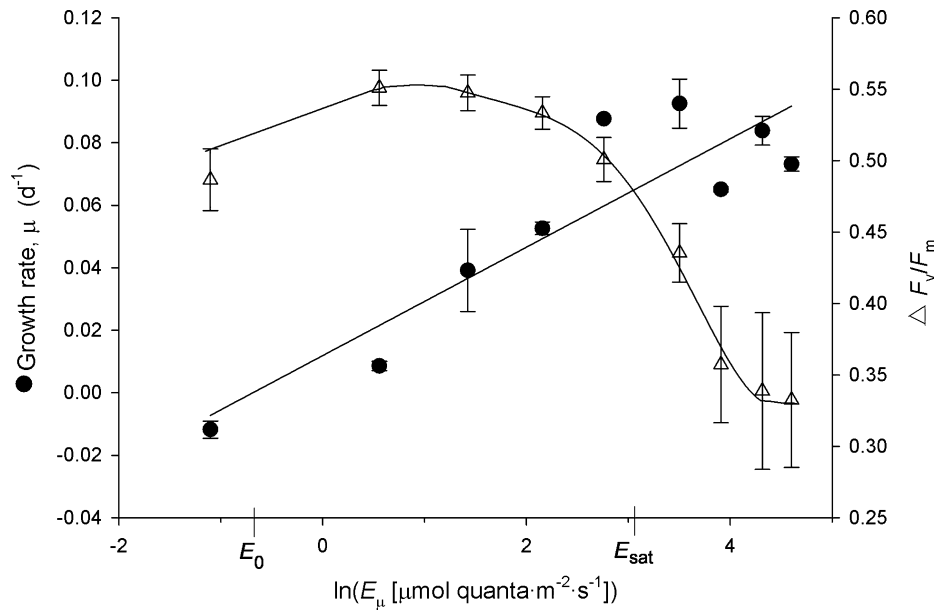
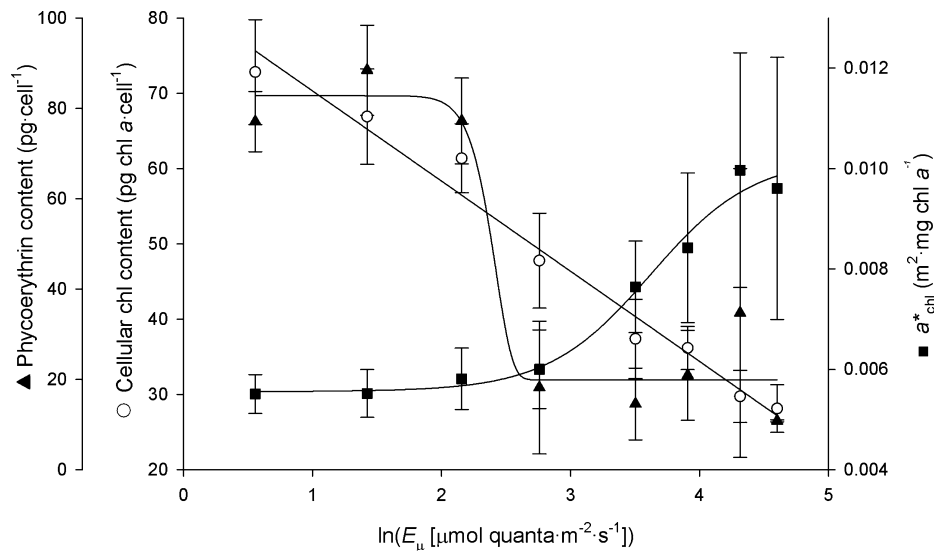


FIG. 2. Phycoerythrin content, chl content, and a_{chl}^* averaged over the course of the experiment for all acclimations showing positive growth rates. Error bars represent standard deviation, $n = 2$. The decrease in chl content was linear with increasing $\ln(\text{growth irradiance})$, while a^* displayed a more complex response. Phycoerythrin is the accessory pigment responsible for *Mesodinium rubrum*'s characteristic red color and is produced by cells under low-light stress.



($P_{\text{max}}^{\text{chl}}$) mirrored growth rate trends, with light-saturated cultures displaying the greatest photosynthetic rates (Fig. 3). In part, high pigment content resulted in self-shading of pigment molecules in light-limited cultures, leading to reduced $P_{\text{max}}^{\text{chl}}$. Cells incubated at $E_{\mu} < E_0$ retained limited photosynthetic capacity. The saturation irradiance for photosynthesis (E_k) increased with increasing E_{μ} ; above E_{sat} , E_k approximated E_{μ} , except for the highest irradiance acclimation ($E_{\mu} = 100 \mu\text{mol quanta} \cdot \text{m}^{-2} \cdot \text{s}^{-1}$), where $E_{k,100} \approx E_{k,75}$ (Fig. 3). For E_{μ} of $16 \mu\text{mol quanta} \cdot \text{m}^{-2} \cdot \text{s}^{-1}$ and lower, $E_{\mu} < E_k$.

Growth efficiency. The quantum yield for growth, ϕ_{μ} , was calculated for cultures with positive growth rates (Table 2). Generally, efficiency declined with increasing acclimation irradiance, so that the quantum requirement for carbon assimilation increased

linearly with increasing irradiance (Fig. 4; $r^2 = 0.96$). The maximum quantum yield for photosynthesis (ϕ_p) showed a similar trend, with light-limited cultures displaying the greatest photosynthetic efficiency (Fig. 4).

DISCUSSION

The results of this study clearly reveal the extraordinary capacity of an Antarctic strain of *M. rubrum* to acclimate to extremely low irradiance. Interpolation of growth-rate data reveals a compensation irradiance of only $0.5 \mu\text{mol quanta} \cdot \text{m}^{-2} \cdot \text{s}^{-1}$. This irradiance not only accurately marks the experimental boundary between negative ($E_{\mu} = 0.33 \mu\text{mol quanta} \cdot \text{m}^{-2} \cdot \text{s}^{-1}$) and positive ($E_{\mu} = 1.7 \mu\text{mol quanta} \cdot \text{m}^{-2} \cdot \text{s}^{-1}$) growth rates but also approximately

TABLE 1. Definitions of abbreviations and symbols used in this text.

Symbol	Definition (and units)
μ	Growth rate (d^{-1})
μ_{avg}	Average observed growth rate (d^{-1})
$\text{Chl } a \cdot \text{cell}^{-1}$	Cellular chl <i>a</i> content ($\text{pg chl } a \cdot \text{cell}^{-1}$)
$\text{C} \cdot \text{cell}^{-1}$	Cellular carbon content ($\text{ng C} \cdot \text{cell}^{-1}$)
$\text{N} \cdot \text{cell}^{-1}$	Cellular nitrogen content ($\text{ng N} \cdot \text{cell}^{-1}$)
E_{μ}	Growth irradiance, acclimation level ($\mu\text{mol quanta} \cdot \text{m}^{-2} \cdot \text{s}^{-1}$)
E_{sat}	Irradiance level at which growth rate saturates ($\mu\text{mol quanta} \cdot \text{m}^{-2} \cdot \text{s}^{-1}$)
E_0	Zero limit for growth, irradiance at which $\mu = 0$ ($\mu\text{mol quanta} \cdot \text{m}^{-2} \cdot \text{s}^{-1}$)
a_{chl}^*	Mean chl <i>a</i> -specific spectral absorption (375–750 nm) ($\text{m}^2 \cdot \text{mg chl } a^{-1}$)
$P_{\text{max}}^{\text{cell}}$	Cellular photosynthetic capacity ($\text{pg C} \cdot \text{cell}^{-1} \cdot \text{h}^{-1}$)
$P_{\text{max}}^{\text{chl}}$	Chl <i>a</i> -specific photosynthetic capacity ($\text{pg C} \cdot \text{pg chl } a^{-1} \cdot \text{h}^{-1}$)
E_k	Irradiance at which photosynthesis saturates ($\mu\text{mol quanta} \cdot \text{m}^{-2} \cdot \text{s}^{-1}$)
Φ_{μ}	Quantum yield for growth ($\text{mol C} \cdot \text{mol quanta absorbed}^{-1}$)

corresponds to the maximum winter irradiance reaching subice waters in saline Antarctic lakes where lacustrine strains of *M. rubrum* overwinter ($0.7 \mu\text{mol quanta} \cdot \text{m}^{-2} \cdot \text{s}^{-1}$; Gibson et al. 1997).

M. rubrum achieves maximal growth rates at a low irradiance compared with other marine phytoplankton, though our experimental values for E_k ranged as high as $75 \mu\text{mol quanta} \cdot \text{m}^{-2} \cdot \text{s}^{-1}$ for the highest light acclimations (Fig. 3). Thus, while they gain no growth-rate advantage, *M. rubrum* cells continue to adjust their photosynthetic apparatus to irradiances above E_{sat} , which likely aids cells in avoiding damage from reactive oxygen species produced by an excess of PAR (Asada 2006). By comparison, E_k for temperate strains of *M. rubrum* may exceed $275 \mu\text{mol quanta} \cdot \text{m}^{-2} \cdot \text{s}^{-1}$ (Stoecker et al. 1991), further indicating a trade-off in the polar strain between exploitation of low-light niches and tolerance of high-light conditions, and compensation for low water temperatures.

Our experiment mimicked light intensities that would be experienced by polar *M. rubrum*, including winter darkness. Extreme low-light conditions ($<0.7 \mu\text{mol quanta} \cdot \text{m}^{-2} \cdot \text{s}^{-1}$, comparable to winter darkness) produced a negative growth subset of cultures, containing unhealthy cell populations of small size, low photosynthetic health, and high a^* values. The latter was the result of low chl *a* $\cdot \text{cell}^{-1}$, which decreased over the course of the experiment, though cells never lost their pigments entirely. Pigment decline may have resulted either from metabolic scavenging of pigments for energetic gains under light-starved conditions or from an inability to replace chl *a* due to a light-requiring step in its biosynthesis. Low $P_{\text{max}}^{\text{cell}}$ and E_k indicate that, while cells were unable to make efficient use of light to

TABLE 2. Experimental growth parameters, averaged over the two experimental replicates.

	0.00	0.33	1.74	4.15	8.6	16	33	50	75	100
E_{μ}										
μ_{avg} ($\times 10^{-2}$)	-0.03 (0.14)	-1.18 (0.273)	0.86 (0.15)	3.91 (1.32)	5.25 (0.203)	8.77 (0.008)	9.25 (0.785)	6.51 (0.083)	8.39 (0.460)	7.32 (0.227)
a_{chl}^* ($\times 10^{-3}$)	9.01 (1.74)	9.99 (2.91)	5.51 (0.389)	5.52 (0.479)	5.81 (0.613)	6.00 (0.784)	7.65 (0.913)	8.42 (1.49)	9.97 (2.34)	9.60 (2.61)
$\text{Chl } a \cdot \text{cell}^{-1}$	38.5 (9.26)	42.0 (11.2)	72.8 (6.98)	66.9 (6.34)	61.4 (4.58)	47.8 (6.31)	37.4 (5.25)	36.2 (2.88)	29.7 (3.46)	28.1 (3.18)
$\text{C} \cdot \text{cell}^{-1}$	1.02 (0.142)	1.09 (0.057)	1.75 (0.307)	1.65 (0.336)	1.52 (0.325)	1.21 (0.126)	1.14 (0.244)	1.76 (0.668)	1.71 (0.623)	1.65 (0.640)
$\text{N} \cdot \text{cell}^{-1}$	0.239 (0.0394)	0.269 (0.0306)	0.394 (0.0839)	0.359 (0.0871)	0.325 (0.0747)	0.262 (0.0364)	0.244 (0.0622)	0.308 (0.105)	0.307 (0.0984)	0.274 (0.0938)
C:N ratio	4.309 (0.308)	4.07 (0.269)	4.47 (0.287)	4.62 (0.229)	4.69 (0.105)	4.66 (0.203)	4.74 (0.380)	5.61 (0.338)	5.48 (0.335)	5.94 (0.342)
Φ_{μ} ($\times 10^{-2}$)	-	-	1.95 (0.987)	3.66 (0.198)	2.31 (0.611)	2.17 (0.166)	0.989 (0.234)	0.591 (0.261)	0.545 (0.312)	0.375 (0.139)

Standard deviations ($n = 2$) are given in parentheses. Data for acclimation irradiances with negative growth rates are given in italics.

FIG. 3. Maximum photosynthetic rates at a range of acclimation irradiances and the saturation point of photosynthesis are plotted against growth irradiance. The line $E_{\mu} = E_k$ is also shown. Data points represent experimental averages \pm standard deviation ($n = 2$). When photosynthetic rate is normalized to chl, the high chl a content of low-irradiance-acclimated cells reduces efficiency of each chl a molecule due to self-shading. Cultures incubated at light intensities below E_0 retained low amounts of photosynthetic capacity in spite of their poor health but were less photosynthetically active overall compared with higher-light acclimations.

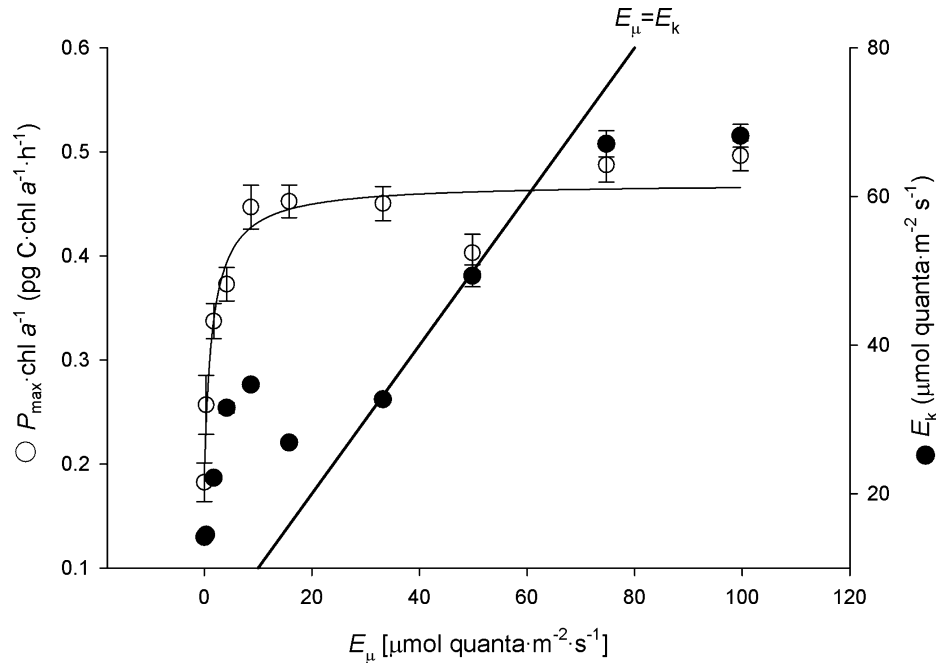
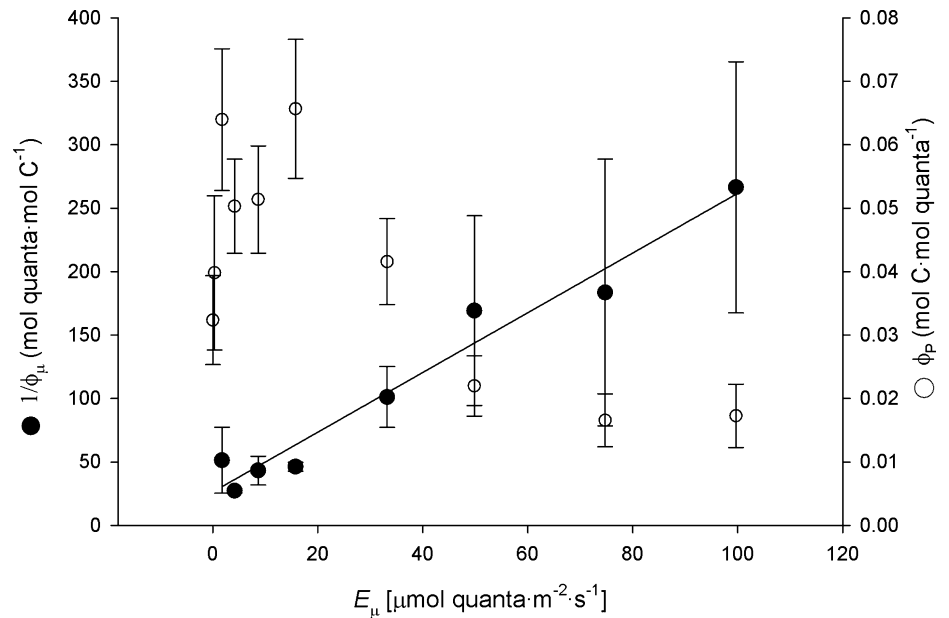


FIG. 4. The inverse of the quantum yield for growth (ϕ_{μ}) calculated according to Falkowski et al. (1985). ϕ_{μ} was calculated only for cultures with positive growth rates. The maximum quantum yield for photosynthesis (ϕ_P) is also shown. Data points indicate mean \pm standard deviation ($n = 2$). The quantum requirement for carbon assimilation increases linearly ($r^2 = 0.96$) with increasing irradiance, indicating that *Mesodinium rubrum* is a less efficient phototroph under high-light conditions. ϕ_P declined with increasing growth irradiance, so that light-limited cultures ($E_{\mu} < E_{\text{sat}}$) were more photosynthetically efficient than their light-saturated counterparts.



fix carbon when temporarily exposed to high-light levels, they were capable of limited photosynthetic activity despite long incubations in near darkness. This result suggests that *M. rubrum* possesses a resilient photosynthetic apparatus adapted to Antarctic winters (see also Johnson and Stoecker 2005).

The maintenance of irradiance-specific chl a levels demonstrates that healthy ($\mu_{\text{avg}} > 0$) *M. rubrum* cells optimize photosynthetic capacity to growth irradiance. Previous research has shown that nuclear-encoded plastid-targeted algal genes are expressed in the ciliate host, and that *M. rubrum* can regulate

plastid division during cell growth (Johnson et al. 2006, 2007). However, the specificity with which the ciliate controls its acclimation response had not yet been demonstrated. Increases in a_{chl}^* and decreases in F_v/F_m indicate a general decrease in photosynthetic efficiency when light is in excess. Together, these data suggest that polar strains of *M. rubrum* acclimate most successfully to low-light conditions and experience light-induced stress when exposed to irradiances $>33 \mu\text{mol quanta} \cdot \text{m}^{-2} \cdot \text{s}^{-1}$.

Carbon-uptake rates also suggest photophysiological distinctions between light-limited and

light-saturated acclimation levels. The parameters P_{\max}^{chl} and a_{chl}^* were smaller in light-limited, pigment-rich acclimations, indicating that cellular response to light is constrained by a packaging effect, in which stacked thylakoids self-shade, reducing the amount of light that reaches each photosystem's antenna (Berner et al. 1989). These changes can also be explained in part by the observed decrease in cellular PE content with increasing irradiance. As in other phototrophs, cellular chl *a* concentrations (and manufacture of accessory pigments such as PE) in *M. rubrum* strike an irradiance-level-specific balance between gains in light harvesting and metabolic costs of maintaining additional photosynthetic capacity. High-light acclimations, by contrast, converged on low photosynthetic efficiency and high P_{\max}^{chl} values, corresponding to high a_{chl}^* . The uniformity of these parameters across the highest irradiance acclimations, despite changes in chl concentration, implies that this *M. rubrum* strain has inherent physiological limitations to growth and photosynthetic rates imposed by its adaptation to Antarctic waters.

Previous researchers have remarked on the slow growth and "poor adaptation" of Antarctic phytoplankton (Jacques 1983, Neale and Priscu 1995), and the additional stress imposed by fluctuations in salinity, temperature, and light availability (Arrigo and Sullivan 1992). Polar *M. rubrum* does indeed have lower μ and P_{\max} than its temperate counterpart. In this experiment, and in previous studies (e.g., Johnson and Stoecker 2005), μ_{\max} was only 0.2 d^{-1} , roughly half of what has been measured in temperate cultures (Yih et al. 2004). However, P_{\max}^{chl} was up to an order of magnitude lower than previous measurements in temperate strains, and P_{\max}^{cell} was only a third of measured values in temperate strains (Smith and Barber 1979, Stoecker et al. 1991). The large discrepancy between temperate and polar photosynthetic rates (relative to growth rates) suggests the Antarctic strain may use its photosynthate more efficiently for growth than temperate *M. rubrum* strains.

Quantum yield for growth and cellular metabolism at low light and temperature. *M. rubrum's* adaptation to low-light and temperature conditions is confirmed by trends in quantum yield for growth. The quantum yield for growth (measured as carbon incorporated per quanta absorbed) is highest at the low-light levels comparable to irradiance in the ciliate's native environment (Fig. 4). At its most efficient, *M. rubrum* uses only 27 photons for every carbon atom it incorporates into biomass. This quantum requirement is comparable to that of temperate diatoms, dinoflagellates, and other "traditional" phytoplankton. *M. rubrum* maintains this efficiency while respiring up to 50% of its photosynthate (Fig. 5), a metabolic cost attributable to its active lifestyle.

The differences in rates between polar and temperate strains of the ciliate demonstrate the importance of temperature in enzyme kinetics. Our

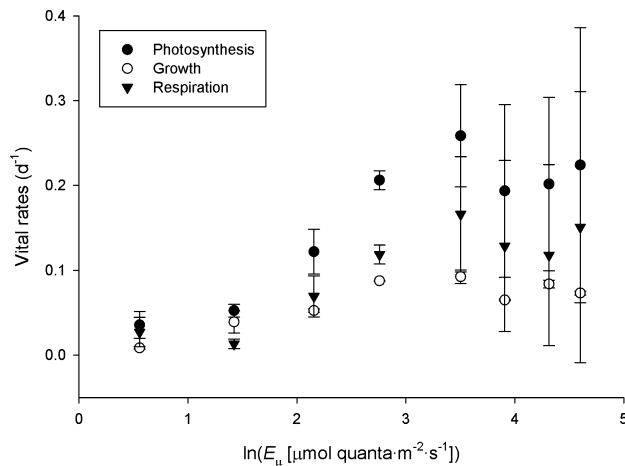


FIG. 5. Comparison of vital rates (mean \pm standard deviation, $n = 2$). Photosynthetic rate was converted to units of d^{-1} using carbon content per cell. Respiration was calculated as the difference between photosynthesis and growth.

measurements of P_{\max}^{chl} fall at the lower end of rates typically observed in polar phytoplankton (Li et al. 1984, Tilzer et al. 1986). Although Q_{10} values of ~ 2 are typical for photosynthetic organisms incubated at varied temperatures for short timescales (Eppley 1972), organisms evolving in cold temperatures may increase their cellular Calvin-cycle enzyme content to counteract the thermal reduction of each enzyme molecule's activity (Li et al. 1984, Davison 1991). Increased chl $a \cdot \text{cell}^{-1}$ at low temperature is a result of oxidation of the plastoquinone pool, which is a signal transduction mechanism for photoacclimation (Escoubas et al. 1995). This phenomenon is opposite to that observed in temperate algae exposed to low temperatures and clearly reveals the ability of *M. rubrum* to not only acclimate to low temperatures but also to become genetically adapted. As in any acclimation strategy, temperature response represents a trade-off between gains in activity and biosynthetic requirements. The Antarctic strain of *M. rubrum* must balance the energetic requirements of maintaining additional active enzymes or chl molecules with marginal benefits at low-light levels. Ultimately, thermal stress may fundamentally limit cellular metabolic capacity.

Our growth-rate measurements confirm the calculation of Johnson et al. (2006) of a Q_{10} of 2.6 for growth. Seasonal changes in measured growth rates of temperate ciliates have been linked to temperature, with Q_{10} values also averaging 2.6 (Nielsen and Kiorboe 1994). Like photosynthesis, growth rate is fundamentally limited by enzyme kinetics, rather than *M. rubrum's* ability to acquire energy and manufacture photosynthetic machinery. While *M. rubrum* has been labeled a functional autotroph in the literature, polar conditions raise questions about the ciliate's mode of nutrition, particularly in winter. Myung et al. (2006) observed increasing rates of

bacterivory with decreasing light levels in a temperate strain of the ciliate. Also, Smith and Barber (1979) demonstrated active uptake of organic compounds in a Peruvian bloom; however, their results may be confounded by the presence of bacteria and other microorganisms in the seawater sample. Research in Antarctic lakes containing *M. rubrum* has demonstrated mixotrophy in other photosynthetic protists, including the cryptophyte *G. cf. cryophila*, which was used as prey in this study (reviewed in Laybourn-Parry 2002).

Though our study confirms a light requirement for growth in the polar strain, the low E_0 suggests that *M. rubrum* may rely on limited heterotrophy during winter stress to supplement its C budget. Mortality rates for cells in complete darkness likely range from 0.001 d^{-1} (measured in the culture incubated at $E_{\mu} = 0 \text{ } \mu\text{mol quanta} \cdot \text{m}^{-2} \cdot \text{s}^{-1}$) to 0.009 d^{-1} (from a fit of all growth rate data), corresponding to a half-life between 693 and 77 d. As our cultures were not axenic, these numbers may represent overestimates of survivorship based on cellular stores from autotrophy alone. Taking the more conservative estimate of a 77 d half-life, overwintering *M. rubrum* populations could be reduced to a quarter or an eighth of their original size. However, individual cells could retain sufficient photosynthetic capacity to resume autotrophy when light returns and conditions are favorable.

Given differences described in μ_{max} and $P_{\text{max}}^{\text{chl}}$ above, bacteria, cryptophytes, and organic compounds may be a more important carbon source for the polar strain than for its temperate counterpart. A mixotrophic strategy, with C source dictated by environmental conditions, can allow *M. rubrum* to survive polar winters while maintaining motility and a minimal photosynthetic apparatus. When light returns, *M. rubrum*'s resilience allows it to be among the first phytoplankton species to respond, while phototrophy frees it from competition with strict heterotrophs. By avoiding encystment in a resting stage and retaining high motility, *M. rubrum* can exploit early windows of opportunity in Antarctic waters.

CONCLUSIONS

The ability of this Antarctic strain of *M. rubrum* to photoacclimate to exceedingly low irradiance levels and its low growth rate, which saturates at only $20 \text{ } \mu\text{mol quanta} \cdot \text{m}^{-2} \cdot \text{s}^{-1}$, indicate its adaptation to thermal and light stress in the polar environment. Though rates of growth and photosynthesis are suppressed by low Antarctic temperatures, the specificity of light adaptation, with convergence on and maintenance at specific cellular chl *a* content, indicates that *M. rubrum* closely regulates its cryptophycean plastids to achieve optimum growth in available light conditions. Differences in cell composition and trends in photosynthetic physiology, a_{chl}^* , and $P_{\text{max}}^{\text{chl}}$ between light-limited and light-saturated acclimation

levels indicate that *M. rubrum* undergoes a transition in photophysiology when growth rate is saturated. Characteristic of this transition is a shift in photosynthetic efficiency: light-limited cells have a larger ϕ_{μ} than light-saturated cells. These trends indicate an upper bound to *M. rubrum*'s adaptive capacity, perhaps evolved concurrently with tolerance of low-light conditions. Though acclimation specificity is expected of phytoplankton, it is nonetheless impressive in *M. rubrum*, which is unable to maintain healthy tertiary endosymbiotic plastids without routine acquisition of cryptophycean nuclei. Our results imply that fine-scale control of acclimation and tolerance of low-light levels enhance niche partitioning and winter survivorship in this polar strain.

We thank Charlotte Fuller for analysis of sample carbon and nitrogen content, Kevin Wyman for laboratory support, and two anonymous reviewers for helpful comments. This research was supported in part by a Barry M. Goldwater Foundation Scholarship and through the Henry Rutgers Scholars Program (H. V. M.), by a Rutgers University institutional postdoctoral fellowship (M. D. J.), and by the National Science Foundation (Grant #0851982 to P. G. F. and M. D. J.).

- Arrigo, K. R. & Sullivan, C. W. 1992. The influence of salinity and temperature covariation on the photophysiological characteristics of Antarctic sea ice macroalgae. *J. Phycol.* 28:746–56.
- Asada, K. 2006. Production and scavenging of reactive oxygen species in chloroplasts and their functions. *Plant Physiol.* 141:391–6.
- Bary, B. M. & Stuckey, R. G. 1950. An occurrence in Wellington Harbour of *Cyclotricium meunieri* Powers, a ciliate causing red water, with some additions to its morphology. *Trans. R. Soc. N. Z.* 78:86–92.
- Berner, T., Dubinsky, Z., Wyman, K. & Falkowski, P. G. 1989. Photoadaptation and the "package" effect in *Dunaliella tertiolecta* (Chlorophyceae). *J. Phycol.* 25:70–8.
- Crawford, D. W. 1989. *Mesodinium rubrum*: the phytoplankton that wasn't. *Mar. Ecol. Prog. Ser.* 58:161–74.
- Davison, I. R. 1991. Environmental effects on algal photosynthesis: temperature. *J. Phycol.* 27:2–8.
- Dubinsky, Z., Berman, T. & Schanz, F. 1984. Field experiments for in situ measurement of photosynthetic efficiency and quantum yield. *J. Plankton Res.* 6:339–49.
- Eppley, R. W. 1972. Temperature and phytoplankton growth in the sea. *Fish. Bull.* 70:1063–85.
- Escoubas, J. M., Lomas, M., LaRoche, J. & Falkowski, P. G. 1995. Light intensity regulation of cab gene transcription is signaled by the redox state of the plastoquinone pool. *Proc. Natl. Acad. Sci. U. S. A.* 92:10237–41.
- Falkowski, P. G., Dubinsky, Z. & Wyman, K. 1985. Growth-irradiance relationships in phytoplankton. *Limnol. Oceanogr.* 30:311–21.
- Falkowski, P. G. & LaRoche, J. 1991. Acclimation to spectral irradiance in algae. *J. Phycol.* 27:8–14.
- Falkowski, P. G., Owens, T. G., Ley, A. C. & Mauzerall, D. C. 1981. Effects of growth irradiance levels on the ratio of reaction centers in two species of marine phytoplankton. *Plant Physiol.* 68:969–73.
- Falkowski, P. G. & Raven, J. A. R. 2007. *Aquatic Photosynthesis*, 2nd ed. Princeton University Press, Princeton, New Jersey, 484 pp.
- Fenchel, T. 1968. On 'red-water' in the Isefjord (inner Danish waters) caused by the ciliate *Mesodinium rubrum*. *Ophelia* 5: 245–53.
- Fujita, Y., Murakami, A., Katunori, A. & Ohki, K. 1994. Short-term and long-term adaptation of the photosynthetic apparatus: homeostatic properties of thylakoids. In Bryant, D. A. [Ed.] *The Molecular Biology of Cyanobacteria*. Kluwer, Dordrecht, the Netherlands, pp. 677–92.

- Fujita, Y., Murakami, A. & Ohki, K. 1990. Regulation of the stoichiometry of thylakoid components in the photosynthetic system of cyanophytes: model experiments showing that control of the synthesis or supply of chl *a* can change the stoichiometric relationship between the two photosystems. *Plant Cell Physiol.* 31:145–53.
- Gibson, J. A. E., Swadling, K. M., Pitman, T. M. & Burton, H. R. 1997. Overwintering populations of *Mesodinium rubrum* (Ciliophora: Haptorida) in lakes of the Vestfold Hills, East Antarctica. *Polar Biol.* 17:175–9.
- Guillard, R. R. L. 1975. Culture of phytoplankton for feeding marine invertebrates. In Smith, W. L. & Chanley, M. H. [Eds.] *Culture of Marine Invertebrate Animals*. Plenum Press, New York, pp. 26–60.
- Gustafson, D. E., Stoecker, D. K., Johnson, M. D., Van Heukelem, W. F. & Sneider, K. 2000. Cryptophyte algae are robbed of their organelles by the marine ciliate *Mesodinium rubrum*. *Nature* 405:1049–52.
- Hansen, P. J. & Fenchel, T. 2006. The bloom-forming symbiont *Mesodinium rubrum* harbours a single permanent endosymbiont. *Mar. Biol. Res.* 2:169–77.
- Harrison, W. G. & Platt, T. 1986. Photosynthesis-irradiance relationships in polar and temperate phytoplankton populations. *Polar Biol.* 5:153–64.
- Hart, T. J. 1934. Red 'water-bloom' in South African seas. *Nature* 134:459–60.
- Jacques, G. 1983. Some ecophysiological aspects of the Antarctic phytoplankton. *Polar Biol.* 2:27–33.
- Jankowski, A. W. 1976. Revision of the classification of the ciliophorids. In Markevich, A. P. & Yu, I. [Eds.] *Materials of the II All-Union Conference of Protozoology. Part I. General Protozoology*. Naukova Dumka, Kiev, Ukraine, pp. 167–8.
- Jassby, A. D. & Platt, T. 1976. Mathematical formulation of the relationship between photosynthesis and light for phytoplankton. *Limnol. Oceanogr.* 21:540–7.
- Jeffrey, S. W. & Humphrey, G. F. 1975. New spectrophotometric equations for determining chlorophylls *a*, *b*, *c*₁, and *c*₂ in higher plants, algae, and natural phytoplankton. *Biochem. Physiol. Pflanz.* 167:191–4.
- Johnson, M. D., Oldach, D., Delwiche, C. F. & Stoecker, D. K. 2007. Retention of transcriptionally active cryptophyte nuclei by the ciliate *Myrionecta rubra*. *Nature* 445:426–8.
- Johnson, M. D. & Stoecker, D. K. 2005. Role of feeding in growth and photophysiology of *Myrionecta rubra*. *Aquat. Microb. Ecol.* 39:303–12.
- Johnson, M. D., Tengs, T., Oldach, D. & Stoecker, D. K. 2006. Sequestration, performance, and functional control of cryptophyte plastids in the ciliate *Myrionecta rubra* (Ciliophora). *J. Phycol.* 42:1235–46.
- Laybourn-Parry, J. 2002. Survival mechanisms in Antarctic lakes. *Philos. Trans. R. Soc. Lond. B Biol. Sci.* 357:863–9.
- Laybourn-Parry, J. & Perriss, S. J. 1995. The role and distribution of the autotrophic ciliate *Mesodinium rubrum* (*Myrionecta rubra*) in three Antarctic saline lakes. *Arch. Hydrobiol.* 135:179–94.
- Li, W. K. W., Smith, J. C. & Platt, T. 1984. Temperature response of photosynthetic capacity and carboxylase activity in Arctic marine phytoplankton. *Mar. Ecol. Prog. Ser.* 17:237–43.
- Lindholm, T. & Mörk, A. C. 1990. Depth maxima of *Mesodinium rubrum* (Lohmann) Hamburger & Buddenbrock—examples from a stratified Baltic Sea Inlet. *Sarsia* 75:53–64.
- Lohmann, H. 1908. Untersuchungen zur Feststellung des vollständigen Gehaltes des Meeres an Plankton. *Wiss. Meer-essunters. Abt. Kiel* 10:129–370.
- Myung, G., Yih, W., Kim, H. S., Park, J. S. & Cho, B. C. 2006. Ingestion of bacterial cells by the marine photosynthetic ciliate *Myrionecta rubra*. *Aquat. Microb. Ecol.* 44:175–80.
- Neale, P. J. & Priscu, J. C. 1995. The photosynthetic apparatus of phytoplankton from a perennially ice-covered Antarctic lake: acclimation to an extreme shade environment. *Plant Cell Physiol.* 36:253–63.
- Nielsen, T. G. & Kiorboe, T. 1994. Regulation of zooplankton biomass and production in a temperate, coastal ecosystem. 2. Ciliates. *Limnol. Oceanogr.* 39:508–19.
- Olli, K. & Seppälä, J. 2001. Vertical niche separation of phytoplankton: large-scale mesocosm experiments. *Mar. Ecol. Prog. Ser.* 217:219–33.
- Owen, R. W., Ganesella-Galvao, S. F. & Kutner, M. B. B. 1992. Discrete, subsurface layers of the autotrophic ciliate *Mesodinium rubrum* off Brazil. *J. Plankton Res.* 14:97–105.
- Parsons, T. R., Maita, Y. & Lalli, C. M. 1984. *A Manual of Chemical and Biological Methods for Seawater Analysis*. Pergamon Press, Oxford, UK, 173 pp.
- Passow, U. 1991. Vertical migration of *Gonyaulax catenata* and *Mesodinium rubrum*. *Mar. Biol.* 110:455–63.
- Perriss, S. J., Laybourn-Parry, J. & Marchant, H. J. 1993. *Mesodinium rubrum* (*Myrionecta rubra*) in an Antarctic brackish lake. *Arch. Hydrobiol.* 128:57–64.
- Powers, P. B. A. 1932. *Cyclotrichium meunieri* sp. nov. (Protozoa, Ciliata); cause of red water in the Gulf of Maine. *Biol. Bull. (Woods Hole)* 63:74–80.
- Robinson, D. H., Kolber, Z. & Sullivan, C. W. 1997. Photophysiology and photoacclimation in surface sea ice algae from McMurdo Sound, Antarctica. *Mar. Ecol. Prog. Ser.* 147:243–56.
- Ryther, J. H. 1967. Occurrence of red-water off Peru. *Nature, Lond.* 214:1318–9.
- Smith, W. O. & Barber, R. T. 1979. A carbon budget for the autotrophic ciliate *Mesodinium rubrum*. *J. Phycol.* 15:27–33.
- Smith, M. & Hansen, P. J. 2007. Interaction between *Mesodinium rubrum* and its prey: importance of prey concentration, irradiance, and pH. *Mar. Ecol. Prog. Ser.* 338:61–70.
- Stoecker, D. K., Putt, M., Davis, L. H. & Michaels, A. E. 1991. Photosynthesis in *Mesodinium rubrum*: species-specific measurements and comparison to community rates. *Mar. Ecol. Prog. Ser.* 73:245–52.
- Sukenik, A., Bennett, J. & Falkowski, P. G. 1988. Changes in the abundance of individual apoproteins of light-harvesting chlorophyll *a/b*-protein complexes of photosystem I and II with growth irradiance in the marine chlorophyte *Dunaliella tertiolecta*. *Biochim. Biophys. Acta* 932:206–15.
- Tilzer, M. M., Elbrachter, M., Gieskes, W. W. & Beese, B. 1986. Light-temperature interactions in the control of photosynthesis in Antarctic phytoplankton. *Polar Biol.* 5:105–11.
- Yih, W., Kim, H. S., Jeong, H. J., Myung, G. & Kim, Y. G. 2004. Ingestion of cryptophyte cells by the marine photosynthetic ciliate *Mesodinium rubrum*. *Aquat. Microb. Ecol.* 36:165–70.